Title

EFFECTS OF NEAR INTERFACIAL MICROSTRUCTURE ON TOUGHNESS AND SUBSCRITICAL CRACK GROWTH IN CERAMIC/METAL SYSTEMS

Authors

Oh, T.S.
Cannon, R.M.
Rodel, J.

Publication Date

1988-02-01

Center for Advanced Materials

CAM

To be presented at the Second International Conference on Composite Interfaces (ICCI-II), Case Western Reserve University, Cleveland, OH, June 13–17, 1988, and to be published in the Proceedings

Effects of Near Interfacial Microstructure on Toughness and Subcritical Crack Growth in Ceramic/Metal Systems

T.S. Oh, R.M. Cannon, J. Rödel, A.M. Glaeser, and R.O. Ritchie

February 1988

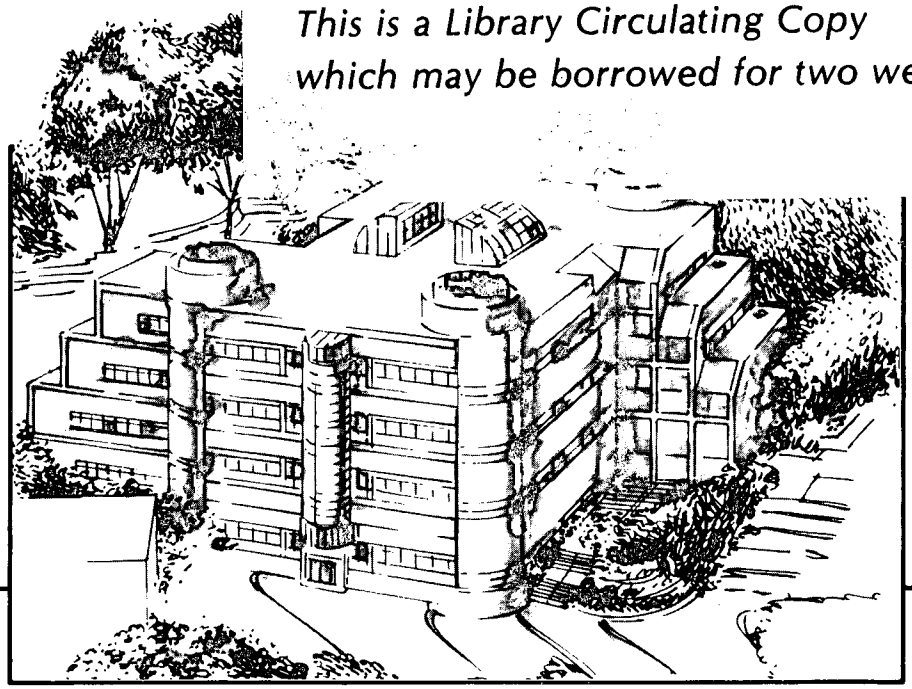

Materials and Chemical Sciences Division

Lawrence Berkeley Laboratory • University of California

ONE CYCLOTRON ROAD, BERKELEY, CA 94720 • (415) 486-4755

Prepared for the U.S. Department of Energy under Contract DE-AC03-76SF00098

DISCLAIMER

LBL-24799

EFFECTS OF NEAR INTERFACIAL MICROSTRUCTURE ON TOUGHNESS AND SUBCRITICAL CRACK GROWTH IN CERAMIC/METAL SYSTEMS

T. S. Oh, R. M. Cannon, J. Rödel, A. M. Glaeser and R. O. Ritchie

Center for Advanced Materials, Materials and Chemical Sciences Division
Lawrence Berkeley Laboratory
and
Department of Materials Science and Mineral Engineering
University of California, Berkeley, CA 94720

February 1988

submitted for proceedings
Second International Conference on Composite Interfaces (ICCI-II)
Case-Western Reserve University
June 13-17, 1988

This work was supported by the Director, Office of Energy Research, Office of Basic Energy Sciences, Materials Sciences Division of the U.S. Department of Energy under Contract No. DE-AC03-76SF00098.

EFFECTS OF NEAR INTERFACIAL MICROSTRUCTURE ON TOUGHNESS AND SUBCRITICAL CRACK GROWTH IN CERAMIC/METAL SYSTEMS

T. S. OH, R. M. CANNON, J. RÖDEL, A. M. GLAESER and R. O. RITCHIE
Center for Advanced Materials, Materials and Chemical Sciences Division, Lawrence Berkeley Laboratory, and Department of Materials Science and Mineral Engineering, University of California, Berkeley, CA 94720

ABSTRACT

Methods to toughen ceramic/metal interfaces that employ prescribed arrays of non-coplanar microcrack-like-voids and inclined interface steps are assessed. These features, developed in glass/copper samples made using photolithographic, metal deposition and diffusion bonding processes, promote crack-tip shielding principally from crack bridging by ligaments generated by plastic void growth within the copper. The ensuing plastic stretching, and sometimes tearing, of the Cu film ligaments yield the major energy dissipation. Crack deflection can also provide a smaller toughening contribution. Resistance-curve (R-curve) behavior obtains from the bridging, with fracture energies rising to an asymptote that varies from 9 to 160 J/m^2, compared with inherent toughness values of $\sim$2 J/m^2 for the specific glass/Cu interfaces used. The arrays retard subcritical crack-growth rates, which are higher in moist atmospheres, by orders of magnitude compared to rates for plain interfaces. The behavior is contrasted with that gained by using better interface chemistry to increase the inherent fracture toughness of glass/Cu bonds.

INTRODUCTION

Robust ceramic-metal adhesion is crucial for components for advanced technologies, such as microelectronic or optical devices, or structures having corrosion, insulating or wear resistant coatings. For example, the potential for interfacial failure within ever larger VLSI chips and multilayer ceramic substrates entails increasingly stringent requirements for the ceramic/metal bonds [1,2]. Optimal adhesion between dissimilar materials is also important for the behavior of ceramic and metal based structural alloys and composites [3-5], albeit in specific instances poor adhesion may enhance toughness [6,7].

To assess the structural integrity of ceramic/metal interfaces, fracture mechanics can be employed to characterize the critical fracture energy, G_c, or toughness, K_c, for interfacial cracking [8-13]. However, loss of a device from interface fracture occurs more often at stresses far below those required for catastrophic failure, from such mechanisms as thermal fatigue or environmentally induced cracking. Thus, to evaluate the reliability of ceramic/metal bonds, it is imperative that both critical and subcritical interfacial crack growth [14] are examined.

The interfacial fracture energy embodies contributions from crack-tip plasticity in the metal and the interfacial bond rupture, that dictate the inherent crack extension resistance, as well as crack-tip shielding mechanisms [12,13]. The latter provide further mechanical and microstructural contributions from mechanisms, such as crack-flank bridging, that enhance macroscopic toughness, or impede crack advance, by lowering the extension

force experienced locally near a crack tip. Efforts to improve interfacial crack-growth resistance have often been directed towards increasing the intrinsic toughness of the ceramic/metal bond by changing interface composition and microstructure [10,15-19]. In the present paper, however, we assess and contrast the benefits of recently reported [20,21] extrinsic shielding mechanisms that utilize out-of-plane microcracking and interfacial geometries to enhance the toughness and subcritical (pre-instability) crack-growth resistance of glass/copper interfaces.

The toughening mechanisms being considered, namely crack bridging and crack bridging plus deflection, are promoted by patterned arrays of non-coplanar microcrack-voids sometimes combined with interfacial steps. These features are generated by etching channels or holes on the surface of glass substrates prior to deposition of metal films and diffusion bonding.

EXPERIMENTAL PROCEDURES

Interfacial fracture was studied using double-cantilever-beam, DB(M_z), specimens, comprised of a thin copper film bonded between silicate glass substrates, with loading grips attached by epoxy (Fig. 1). As described elsewhere [12,14,19], specimens were made by evaporating Cu films onto two substrates (of size 75 by 25 by 2 mm), and pressure diffusion bonding the two layers together in vacuum. Bonding temperatures of 400°C and above were used for reference samples, whereas only 450°C was used for toughened samples to avoid fracture in the glass. To confine fracture to one interface, a 10 to 20-nm layer of chromium was evaporated onto the other substrate prior to depositing the Cu. Mechanically masking to limit the deposition area yielded a thin pre-crack and side grooves when desired.

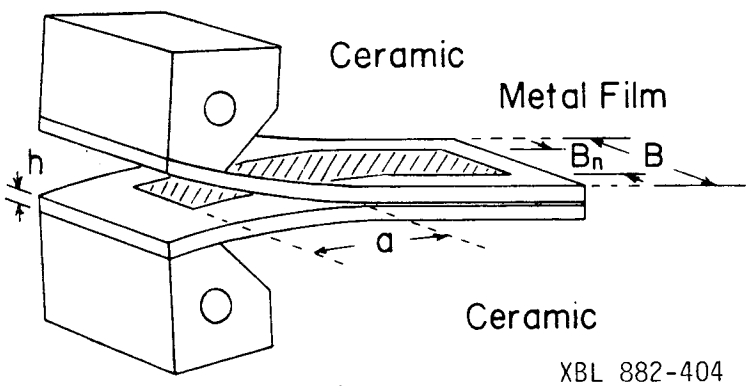

Fig. 1. Schematic of sandwich type, double-cantilever-beam, DB(M_z), specimen used to evaluate crack growth behavior along glass/Cu interfaces.

To assess the effects of interfacial morphology and nearby microcracks on interfacial fracture, periodic arrays of long channels or of round (pill-box) holes were etched into the glass substrate prior to film deposition and bonding using a photolithographic technique described in refs [20-22]. A positive photoresist layer was exposed, developed, and cured to produce the desired pattern on a specific strip of substrate prior to etching either with 10% hydrofluoric acid solution or an argon ion beam. Although ion etching can produce more uniform and finer patterns [23], the photoresist organics are difficult to remove after reactions induced by ion bombardment. Moreover, for present purposes, chemical etching in HF may be preferable as it increased the microroughness of the substrate surface [24]. Photomask images were designed to produce 782 parallel channels on the substrate, of

size 16 μm x 25 mm spaced on 32 μm centers, or else 280,000 round holes of 8 or 16 μm diameter, arrayed on a square grid with 16 or 32 μm, respectively, between centers. Due to pattern broadening from over-exposure and undercutting during etching, however, actual arrays consisted of rather larger (25-45%) channel widths or hole diameters but having the prescribed center-to-center spacing. Etching times were controlled to produce channels or holes 1.5-3 μm deep on the substrate.

Test specimens containing specified arrays of near-interface microcrack-voids, with various void and interface geometries, depicted in Fig. 2, were made by combining a patterned and a plain glass substrate and employing the metal deposition and bonding sequence described. Microcrack-like-voids remain in the copper owing to constrained deformation of the thin metal during bonding. The proximity to the interface of these microcracks, which dictates the thickness of bridging ligaments generated by them, was varied by adjusting the amount of Cu put onto each side. As one interface contains a stronger chromium layer, crack extension occurs along the glass/copper interface opposite the Cr deposition. Thus, to generate only crack bridging, Fig. 2a, a copper film, evaporated onto a plain substrate, was bonded to a Cu film on a patterned substrate containing a prior 10 to 20 nm chromium layer. To promote crack bridging plus deflection, Fig. 2b, Cu films were similarly formed, but with the plain substrate having the prior Cr layer. The total metal thickness was 1.1 to 2.3 μm. Having etched arrays within only part of the sample allowed assessment of the inherent toughness, G_o, for fracture along the plain interface without adjacent microcracks and, then, of the resistance-curve (R-curve) development.

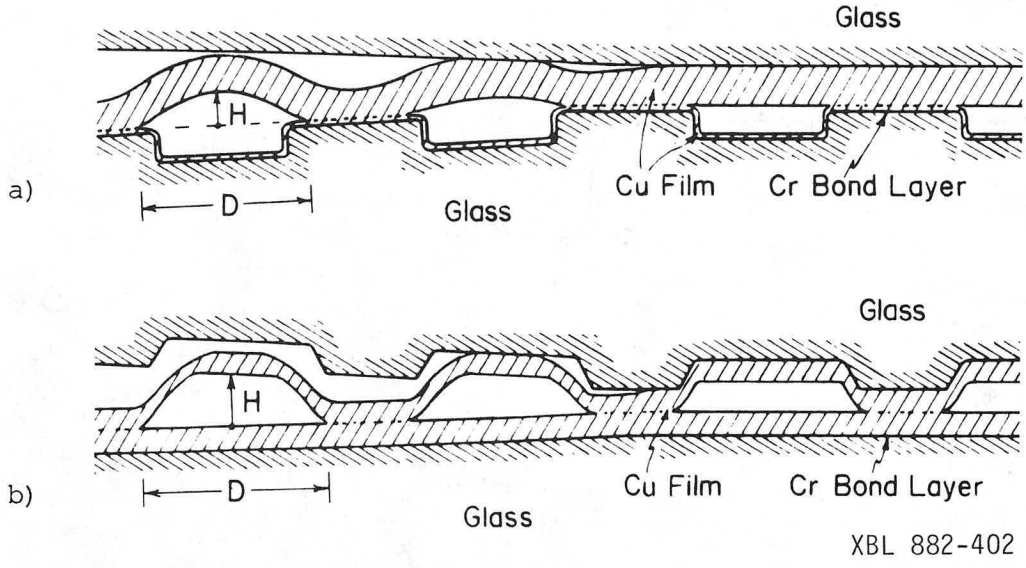

Fig. 2. Configurations that provide out-of-plane microcracks, which induce crack bridging, and interface tilts, which cause deflection. Fracture is obtained along one, designated glass/Cu interface by emplacing a Cr bond layer on the interface across the film. Thus, alternating placement of this chromium layer leads to specimens which experience: a) only bridging with extension along a flat glass/Cu interface, or b) bridging plus deflection via extension on a patterned glass/Cu interface.

Crack extension forces are expressed in terms of both the strain-energy release rate G, and stress-intensity factor, K. Values of G were computed from handbook solutions in terms of the crack length a, gross specimen thickness B, crack-front thickness B_n, and half-height h, as [25,26]:

$$G = \frac{12(Pa)^2(1-\nu^2)}{Eh^3BB_n}\left[1 + \frac{2}{3}\frac{h}{a}\right]^2 \quad , \qquad (1)$$

where E and ν are, respectively, Young's modulus and Poisson's ratio for the glass. (The plane-strain condition obtains because the plate-like geometry and grips preclude anticlastic curvature.) Although the elastic modulus mismatch of copper and glass across the interface causes some shear loading on the crack plane and further stress-field perturbations very near the crack tip [27], with the nearly symmetrical test configuration and thin metal film used herein, the stress-field rotation is minimized and loading is almost purely tensile at the crack tip. Approximate values of K were thus computed as if for a homogeneous material from $(GE/(1-\nu^2))^{0.5}$. Eq. 1 can be regarded as nearly exact as the elastic strain energy is largely contained within the thicker glass arms, and is thus insensitive to modifications in the stress-field singularity near the crack tip due to local deformation in the metal film or to elastic discontinuities.

Fracture toughness was assessed at a constant cross-head speed, whereas subcritical crack-growth tests were conducted under fixed displacement conditions described in ref. 14. The latter were performed using a polyethelene environmental chamber, which was fed continuously with desired mixtures of "dry" ($\sim$ 0.1% relative humidity) or "wet" ($\sim$100% humidity) gases, obtained by passing gaseous nitrogen through, respectively, a liquid nitrogen cold-trap or a water column. Crack positions, denoted by interference fringes seen through the glass, were monitored visually or with a 10X traveling microscope at low crack velocities, da/dt.

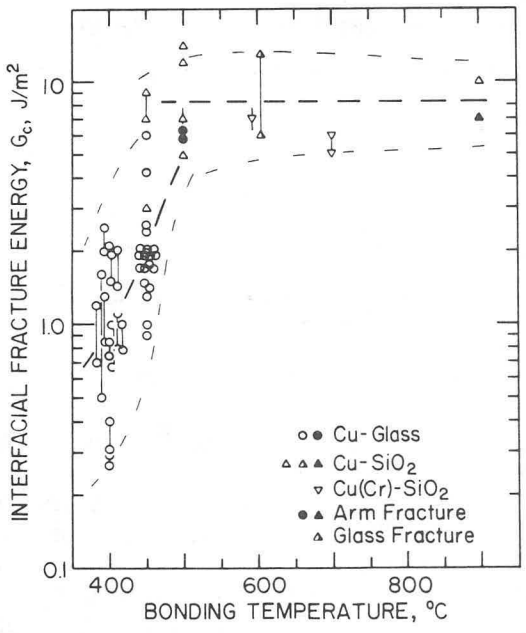

XBL 882-402

Fig. 3. Effect of annealing on the fracture energy of plain interfaces of glass/copper made from soda-lime glass or fused silica. The values for soda-lime glass bonded at 450°C serve as a reference for the subsequent toughened samples, [ref. 19].

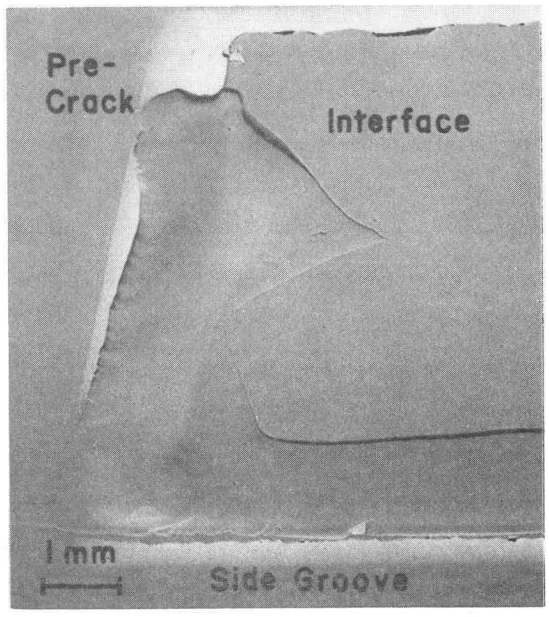

XBB 882-1041

Fig. 4. Scanning electron fractograph of well-bonded silica/Cu sample (500°C) for which initial crack advance was largely in the glass. Subsequently, extension was along the interface except for one strip wherein glass fracture persisted.

RESULTS

Reference Interfaces

Diffusion bonding the copper at 450°C and using soda-lime glass, as was done for the toughened samples, yields an inherent toughness for these plain glass/copper interfaces, G_o, of ~ 2 J/m^2, as shown in Fig. 3 from results of various [13,14,19-21] experiments. These toughnesses exhibit variability with processing, but little systematic change with crack extension. The fracture occurs exactly at the interface as detected by optical and electron microscopy [19] and affirmed by preliminary results of examination of the fracture surfaces with Auger spectroscopy [28].

These interfacial fracture energies increase with copper bonding temperature, presumably owing largely to dispersal of interfacial impurities, left from preparation, by diffusion into the copper and glass during the anneal, Fig. 3, [19]. For bonding temperatures of 500°C and above, the fracture energy using silica is much higher, about 10 J/m^2, and is comparable to that of glass. For these, the glass arms fracture without the use of side grooves; with deep side grooves (B_n/B = 1/3), fracture more often occurs along the interface, but sometimes "plucks-out" pieces of glass, or occasionally runs parallel to the interface within the glass, Fig. 4.

Table I. Sample Geometries and Resultant Fracture Toughnesss

Spec. No.	Cracking Interface	Etching Method	Etched Geometry	Etched Depth (μm)	Bulge Film Thickness[1] (μm)	G_o[2] (J/m^2)	ΔG_c[3] (J/m^2)
1	Plain	Ion	20 μm Channels	1.5	1.5	2	6
2	Plain	HF	22 μm Channels	1.5	1.2	(∿2)	7/8
3	Plain	Ion	20 μm Channels	1.5	1.1	1.5	7
4	Plain	HF	22 μm Channels	1.5	0.75	1.4	8/10
5	Plain	Ion	20 μm Channels	1.5	0.4	3.1	8
6	Patterned (smooth)	Ion	20 μm Channels	1.5	0.75	2.6	8
7	Patterned (microrough)	HF	22 μm Channels	1.5	0.75	1.7	10/13
8	Patterned (microrough)	HF	22 μm Channels	1.5	0.75	1.4	9
9	Patterned (microrough)	HF	23 μm Pennies	1.5	0.75	2.1	7
10	Patterned (microrough)	HF	10 μm Pill boxes	3	0.75	(∿2)	160

[1]Thickness of copper between the microcrack-pore and the cracking interface.
[2]G_o is the inherent interfacial fracture energy of the plain interface.
[3]ΔG_c is the steady state/maximum increase in fracture energy due to crack-tip shielding.

Toughened Interfaces

In the presence of the patterned arrays, the toughnesses increased by factors of 4 to 80 times G_o for the glass-Cu interfaces used, and often markedly exceeded the inherent toughness of bulk glass. Table I describes various configurations used and resulting toughness increases, ΔG_c, [20,21].

Almost all of the toughened samples (except 10 and 5) exhibited complete interfacial fracture. Scanning electron microscope (SEM) fractographs of resulting copper surfaces, in Fig. 5, and cross-sections of a crack-path profile, presented in Fig. 6, illustrate that the patterned regions contain a regular array of microcrack-like-voids within the copper film, and that the segments of Cu films adjacent such microcracks are stretched and bulge considerably during passage of the interfacial crack.

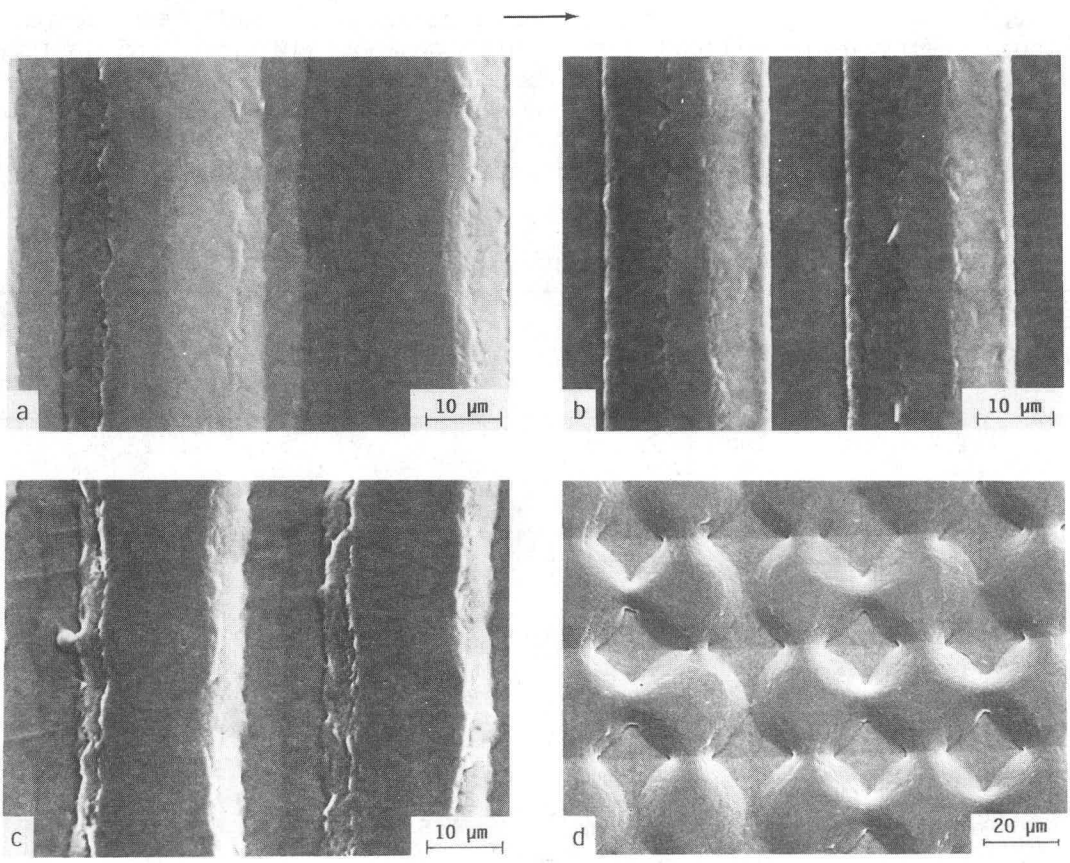

XBB 879-7919B

Fig. 5. SEM images of metal surface from interface fractures comparing bulges for: a) fracture on a plain interface, specimen #4; fracture along patterned interfaces for b) ion etched specimen #6, and c) rougher, HF etched specimen #7; and d) specimen with round bulges, #9 (see Table I for key) [refs. 20,21]. Arrow indicates crack growth direction.

Representative plots of fracture energy expended during crack extension are shown in Fig. 7 for specimens that experienced complete interfacial fracture. As the interfacial cracks traverse the patterned regions, rising R-curves are manifest, with the maximum toughness attaining G_c values of between 9 and 15 J/m^2. After the cracks pass the patterned regions, fracture energies drop abruptly, apparently reverting to G_o.

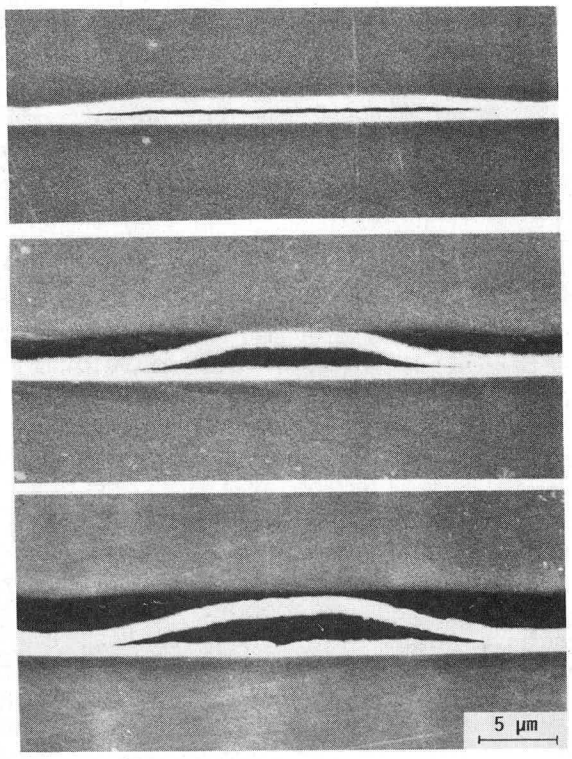

XBB 882-937

Fig. 6. Sequence of events during crack extension is illustrated by SEM images of cross-sections revealing crack path for a chemically etched specimen fracturing along a patterned interface showing: (top) prior microcrack ahead of the main crack, (center) partial development of bridging bulge via lateral growth of a microcrack, and (bottom) fully developed bulge after separation from glass.

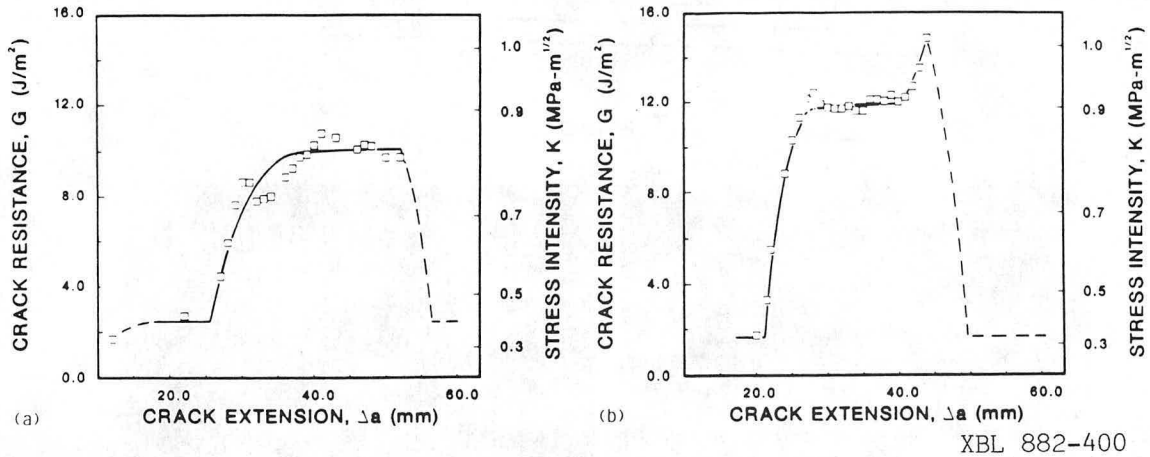

XBL 882-400

Fig. 7. Interfacial fracture-toughness represented as G vs. Δa resistance curves for a) ion etched specimen, #6, and b) HF etched sample, #7, [21].

Several aspects of the R-curves for fracture that followed the intended interface merit comment. First, the R-curves rise to a plateau, apparently attaining a steady state, but for HF-etched samples, a second transient rise in toughness usually occurs as the crack approaches the end of the patterned region (Fig. 7b). Second, channel-type specimens give nearly comparable toughness increases (Table I) where the crack is driven along the plain, deflection-free interface (e.g., specimen #4), and where the crack follows the patterned interface (specimens #6-8), wherein toughening derives from both crack deflection and bridging. Third, for fracture along patterned interfaces (Fig. 2b), chemically-etched glass/Cu interfaces (e.g., #7) exhibit more steeply rising R-curves and slightly greater increases in plateau toughness compared to comparable ion beam etched glass/copper interfaces (#6), behavior which appears to derive, in part, from increased microroughness of substrate surfaces following HF etching (c.f., Figs. 5b & 5c).

Evidently crack bridging is the dominant crack-tip shielding mechanism in toughening the interface, but HF etching imparts some benefits.

In HF-etched samples, some undercutting, apparently involving acid having wet under the photoresist, often lowers the entire flat of the glass between channels. (This causes the regularly spaced lines between bulged copper segments on the fracture surfaces in Figs. 5c & 5d). Such undercutting is apparently responsible for the peak in toughness above the plateau of the R-curve, shown in Fig. 7b. This undercutting causes a region of poor diffusion bonding at the edges of the patterned region. Most importantly, as the main crack approaches the end of the patterned array, greater stretching of the individual metal bulges occurs for an uncertain reason [21]. In addition, the Cu film tears as the crack diverts through the poor diffusion bond. With ion etching, however, such undercutting, and the resultant local toughness peak on the R-curve are absent (Fig. 7a). The poorly bonded region at the start of the arrays may similarly accelerate the rise in the R-curve for HF-etched samples.

Finally, in sample 1Ø fracture involved tearing many of the bridging Cu ligaments, leaving copper segments within the etched holes in the glass fracture surface, as shown in Fig. 8. The exceptional toughness, $\sim$160 J/m^2, evidently arose from the large deformation of the copper. Specimen 5, which had a very thin bridging film, also exhibited appreciable tearing in places.

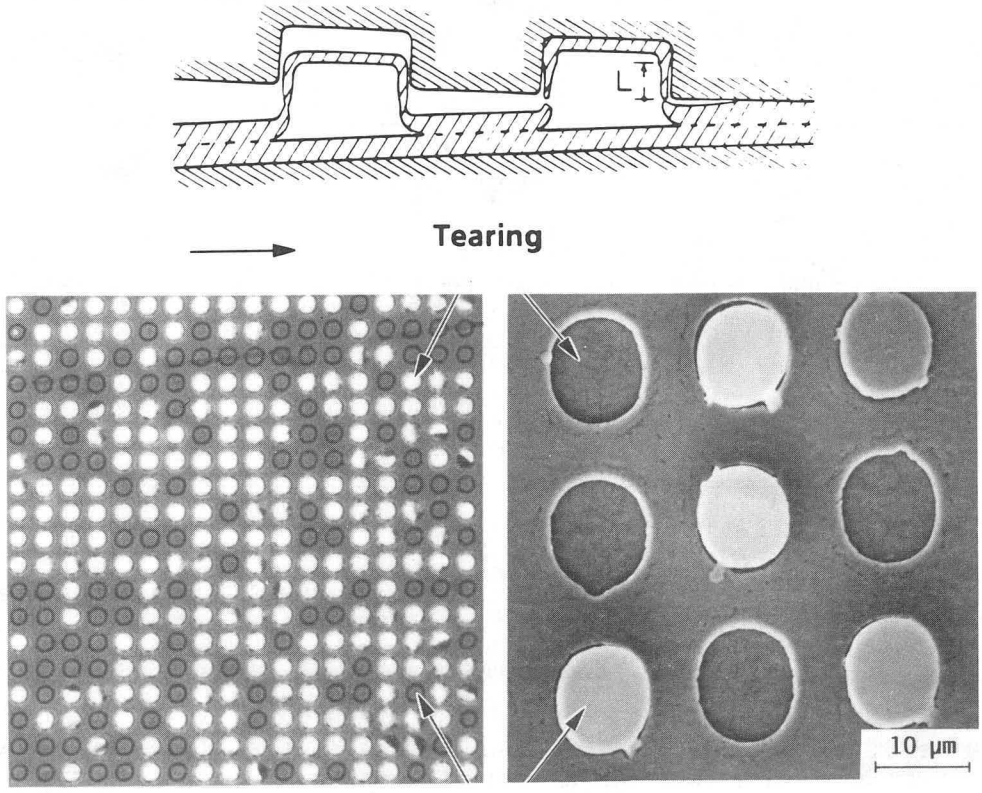

Fig. 8. Schematic of crack path and a) optical fractograph of glass surface and b) SEM fractograph of Cu surface for sample #1Ø showing tearing of most of the Cu bridges that led to $G_c \sim 160$ J/m^2. Arrow shows crack growth direction [ref. 2Ø].

Subcritical Crack Growth

The resistances of plain and toughened glass/copper interfaces to stress-corrosion cracking are compared in Fig. 9, where subcritical crack-growth rates, da/dt, spanning a wide velocity range, are plotted as a function of crack-extension force for both dry and moist environments. As discussed previously [14], interfacial growth rates are extremely sensitive to the presence of moisture. With 450°C bonding, interfacial crack velocities with soda-lime glass exceed by far those measured [29] for bulk soda-lime glass. For a silica/Cu sample annealed at higher temperature, resulting in higher inherent interfacial toughness, the subcritical cracking resistance is markedly improved (Fig. 9a) and is comparable or superior to that of either bulk glass [29].

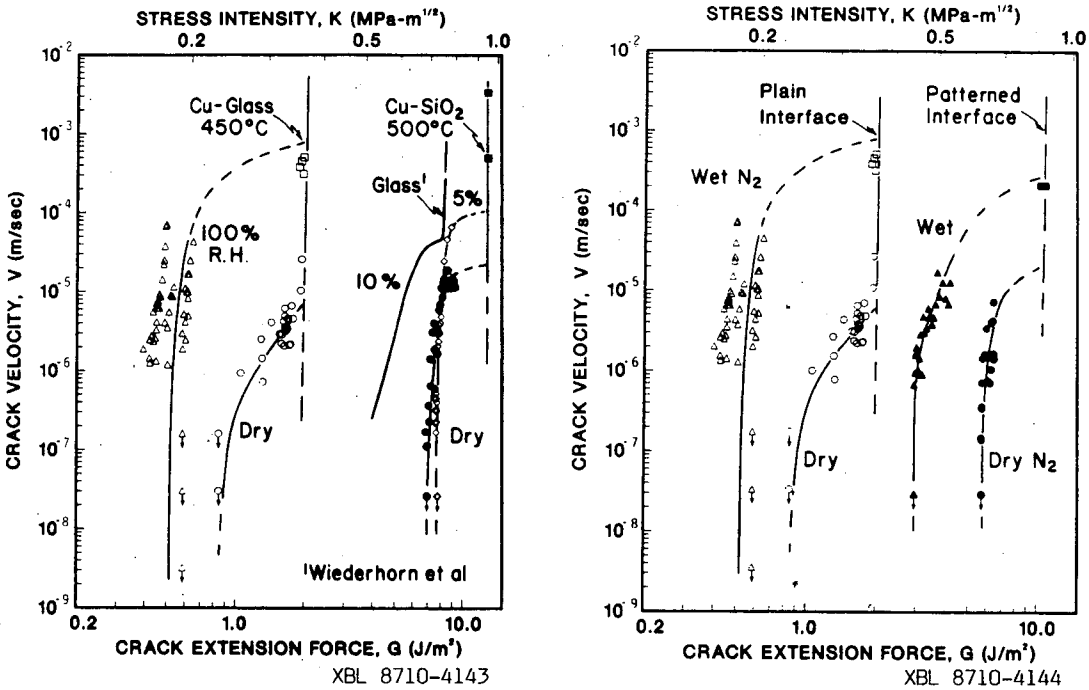

Fig. 9. Variation in subcritical crack-growth rates (da/dt) along glass/Cu interfaces as a function of crack extension force in moist and dry gaseous nitrogen: a) compares behavior for plain interfaces bonded at 450 and at 500°C, the latter giving greater inherent fracture resistance [19]; b) compares plain and toughened interfaces (specimen #8), both bonded at 450°C [21]. Note how the presence of arrays of microcrack-voids near the interface results in far lower crack speeds and a 6 to 7-fold increase in both threshold fracture energy and G_c for interfacial fracture.

Subcritical crack-growth rates in a sample with a patterned interface (prepared by chemical etching) are orders of magnitude lower than with only comparable plain interfaces (Fig. 9b). Moreover, the toughened interfaces show threshold interfacial fracture energies, below which crack growth is presumed dormant, which are increased by a factor of 6 to 7 compared to those for similar plain interfaces. The form of the v-G curves and the specific influence of moisture, however, is similar.

Fractographs of the copper side of the cracked interface indicate progressively less plastic stretching of the bulged metal film (bridging

ligaments) obtains with increasing relative humidity or decreasing crack velocity, as is illustrated by profilometer traces across the fracture surfaces in Fig. 10. This can be attributed to a weakening of interfacial bonds by adsorbing water molecules, which effectively reduces shielding by limiting the extent of stretching of the metal film during crack passage.

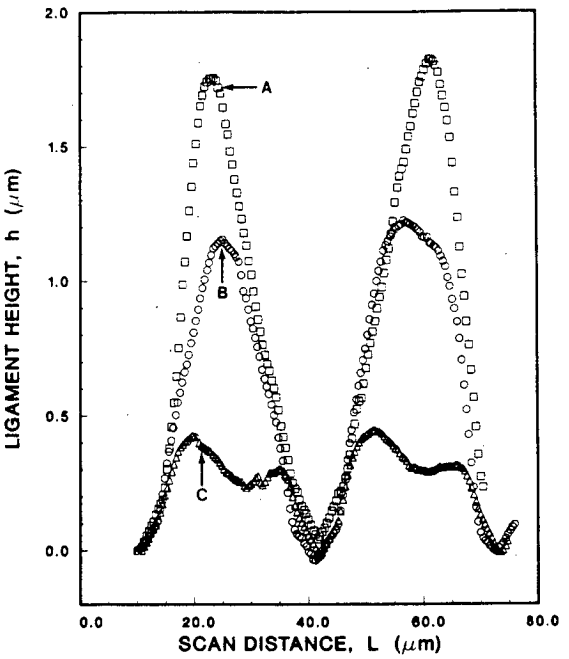

XBL 882-403

Fig. 10. Profilometer traces across a Cu fracture surface from regions of A) virtual instability at G_c and subcritical crack growth at lower G in B) dry and C) wet atmosphere, corresponding to data in Fig. 9b, specimen #8. The heights of bulged metal films and associated plastic stretching are reduced with increased severity of environment (although the absolute heights are depressed relative to microscopic measurements owing to the weight of the stylus, e.g., compare with Fig. 6c).

DISCUSSION

The present results demonstrate that implanting periodic arrays of microcracks/voids adjacent to ceramic/metal interfaces can markedly increase the fracture toughness of the interface. Fractography has affirmed that the toughening mechanism involves crack bridging. Specifically, plastic deformation of bulged segments of copper film, which bridge the crack behind its tip, evidently produces the main energy dissipation, for crack extension along either the plain or patterned side of the metal film, Figs. 2a or 2b. The bridged ligaments of metal film, which are triggered by the implanted microcracks and remain attached to the glass adjacent to the microcracks, impose closure forces on the crack surfaces and thereby reduce the crack-tip opening stresses at the leading cracks.

The uniform array of "microcracks", which are out-of-plane to the main crack, perturb the stress field, causing stress relaxation in unconstrained segments of copper film adjacent to microcracks and so at the tip of an approaching interface crack. With applied stress, microcracks coplanar to the main crack are initiated on the constrained portions of the interface (Fig. 2), leaving metal film ligaments intact with the glass. With progressively increasing applied stress, the metal film (bridging) ligaments in the crack wake are plastically stretched (Fig. 6b), before final linkage of the coplanar microcracks by complete interfacial fracture (Fig. 6c) or alternatively by tearing of copper film, specifically when it is stretched beyond its fracture ductility.

Although that description applies with the continuous void channels parallel to the crack front, for extension with penny-shaped, out-of-plane microcracks (specimen 9, Fig. 5d), the main crack can bow between the pinned segments and then reconnect without having to nucleate new co-planar microcracks each time the crack front advances past another subsurface microcrack

(Fig. 2). Although neither was optimized, these two pore geometries yielded roughly comparable results, suggesting that the latter differences are of secondary importance here, and that stretching of the bridged metal film provides the primary toughening.

Based upon this perception, the R-curve toughness behavior with the microcrack arrays (Fig. 7) is attributable to the development of a bridged zone in the wake of the crack front. As the crack advances into a patterned region, the toughness increases with increasing size of the bridged zone (i.e., number of bridging ligaments) until a steady-state toughness is attained, wherein load-bearing capacity obtained with newly-formed ligaments coincides with that lost due to the fracture of glass/copper bonds between stretched ligaments far behind the tip.

The steady-state toughening can be estimated by recognizing that the incremental stretching of all the ligaments while the crack extends one period, λ, is equivalent to creating one complete bulge. Thus, if an area fraction, X, bulges and experiences an average plastic strain ε_p in going from inception to severence, the work per unit crack area is $X\sigma_y\varepsilon_p t$ where σ_y is the average flow stress and t the thickness of stretched metal film. Approximating the final bulge as an arc of height H and width D, as in Fig. 2, gives the increase in toughness, ΔG_c, as:

$$\Delta G_c = \sigma_y \cdot t \cdot (8X/3)(H/D)^2 \quad , \tag{2}$$

Using measurements for channel arrays of a microcrack length of D $\sim$ 22 μm, a stretched film height of H $\sim$ 5 μm and thickness t $\sim$ 0.65 μm, and a segment spacing of $\lambda \sim$ 32 μm giving $X = d/\lambda \sim 0.7$, and then taking the flow stress of the copper film to be $\sim$200 MPa [30], Eq. 2 yields $\Delta G_c \sim 12$ J/m^2. A somewhat lower ΔG_c value obtains for the discrete pore array (Fig. 5d) for which X is smaller. These agree satisfactorily with experimental results in Table I for samples with complete interface fracture.

The toughness increment is dictated, in part, by a competition between severing the bridging bulges by interfacial fracture and further stretching the ligaments. For example, fractography (Fig. 10) revealed that the extent of ligament stretching and resultant toughening is diminished when local resistance to interfacial fracture, G_o, is reduced by chemical means, during subcritical cracking. In addition, the small tendency toward greater toughening with diminished film thickness, specimens 1 through 5, which runs counter to the explicit trend in Eq. 2, presumably arises because thinner films can be stretched further. In the limit of sufficient interfacial fracture resistance, the bridging ligament may tear instead, as was obtained in the toughest sample (Fig. 8). In such instances, the toughening increment can be estimated as:

$$\Delta G_c = \sigma_y \cdot X_f \cdot u_c \tag{3}$$

where u_c is the critical crack opening for fracture of the bridging copper ligaments, and X_f the area fraction so torn. If a short ligament of film of length, L, debonds and stretches to ε_f prior to fracture, then $u_c \sim \varepsilon_f L$. Taking the average flow stress to failure as 500 MPa, and $\varepsilon_f = 0.5$, and with $X_f \sim \pi Dt/\lambda^2 \sim 0.12$ with $\lambda \sim 16$ μm, the spacing between pores in the square array, Fig. 8, implies a seemingly plausible debond length of 5 μm to account for the $\sim$160 J/m^2 observed for sample 10. Although specimen #5 also experienced some film tearing, the much lower toughness can be ascribed primarily to the very much smaller area fraction of bridging film, i.e., $X_f \sim 2t/\lambda \sim 0.02$.

Further toughening may arise, in principle, from crack-tip deflection at the etched steps for fracture along the patterned interfaces. Although

deflection effects are inadequately understood, the augmented toughness from these steps has been estimated using two models (derived in refs. 31 & 32) for idealized two-dimensional cracks with repeated, kinked segments. Based on measurements of the steepest incline of the interfacial crack-path geometries used for channel arrays (Fig. 6, 35 deg), toughness increases were found to be minimal (i.e., Ø.Ø1 and Ø.2 of G_o for the bounding estimates or Ø.Ø2 to Ø.4 J/m^2) [21], consistent with the similarity in ΔG_c between specimens #4 and #6. Greater effects would be predicted, however, if deflected cracks exhibit a higher G_o under the mixed mode loading experienced on the inclines.

The results (Table I) suggest that cracking along a surface roughened from chemical etching (e.g., Fig. 5c) leads to 1Ø-2Ø% greater steady-state (plateau) toughness than when the crack proceeds along a smooth interface. Such an hypothesis is consistent with reports for silica containing ceramics that hydrofluoric acid etching improves ceramic/metal adhesion by increasing the surface micro-roughness [24], and that surface pitting from boiling acids or molten alkali enhances alumina/copper bond strengths [33,34]. This toughening increment far exceeds the trivial additive contribution discussed above for the tilted interfacial steps. The apparently stronger effect of the very fine scale surface roughness is considered to arise, in part, because the required tilt and twist cause a greater decrease in local crack extension force on the tip [35]. This not only inhibits extension of the interfacial crack but, in turn, induces greater plastic stretching of the bridging metal ligaments as the main crack extends. A greater benefit from the pattern-etched steps may acrue if a steeper or longer incline would cause further stretching, even tearing of the film, such as occurred in specimen 1Ø, Fig. 8.

Thus, the prescription that emerges suggests that a combination of enhanced G_o and interface deflection be used to enable stretching to failure of bridging films with greater thicknesses and cross-sectional areas, but without utilizing high enough interfacial bonding to divert the crack into the glass. Appreciably higher values of ΔG_c than either of those associated with ligament fracture are thereby to be expected with such refinement.

Although the discussion has been in terms of bridging, the toughening mechanism can be viewed, alternatively, as shielding derived from lateral growth of microcrack-voids in a damage zone ahead of the "crack-tip" which is then associated with the point of crack continuity, i.e. of failure of the last bridging ligament [36]. The present work highlights this equivalence and conclusively demonstrates the positive shielding effects from a frontal, plastic microcrack zone, effects which are commonly masked by the countervailing degradation of the main crack path by the microcracks. This adverse aspect does not occur herein as the microcracks are in the tougher metal and, by their lateral growth, shield the inherently weaker interface which is presently not degraded by preexistant microcracks.

It should be clear that this mechanism is applicable to toughening thin film or adhesive joints, but also to single ceramic/metal interfaces if out-of-plane microvoids can be produced in the ductile phase suitably near the interface. The tougher chromium bond layer is not needed to promote crack bridging, but merely assists investigation by keeping the crack at the one, desired interface. This is illustrated by earlier results with film configurations showing that when both interfaces are nominally identical, unidentified heterogeneities can promote local decohesion at both glass/Cu interfaces leading to uncontrolled bridging and substantial toughening [12,13]. This method may also be applicable for materials such as bonded carbides where alternating interfacial decohesion and/or void growth within the metal interlayers could enhance the fracture toughness.

Adjustments in interfacial chemistry, such as obtained via annealing (Fig. 3) can appreciably raise the inherent toughness of glass/metal interfaces, i.e., to G_c values exceeding 10 J/m^2. However, that approach can entail high enough crack-tip stresses to promote fracture in the brittle glass [19], particularly with the use of a hard Cr bond layer wherein the yield stresses are high and crack-tip plasticity minimal [37,13]. In contrast, the microcrack induced bridging yields toughening by virtue of spreading the damage, leading to toughnesses comparable to or far exceeding those for glass [29,38] (i.e., 9 J/m^2) but with no fracture of the ceramic. An adverse aspect is that peak toughness only develops after enough crack extension to develop a bridging zone. However, similar toughening has been observed in association with submicron sized bulges [12], implying that with suitable geometrical modifications, good fracture resistance could obtain for much smaller cracks and crack extensions than those found here. With such changes, this mechanism should be of benefit in microelectronic applications where fracture of the brittle semiconductor or ceramic is a common failure mode for wire bonds or interconnects. This mechanism may also pertain for fiber composites wherein suitably defective films of metal along fiber interfaces could forestall fiber fracture and lead to energy dissipation via growth of bridged cracks along the fibers.

CONCLUSIONS

Results presented have illustrated mechanisms, based on controlled interfacial geometries and out-of-plane microcrack-voids made by photolithographic methods combined with metal deposition and diffusion bonding processes, that extensively toughen ceramic/metal interfaces via crack bridging. Moreover, although the method has been demonstrated for toughening thin-film, sandwich joints, it should also pertain for toughening any ceramic/metal interface for which suitable out-of-plane defects can be formed. The critical aspects are:

1. The fracture resistance of glass/copper interfaces is enhanced by the presence of controlled arrays of microcrack-voids, emplaced out-of-plane to the main crack. The presence of such near-interface "defects" relaxes stresses in segments of the Cu film adjacent to the "microcracks"; their lateral growth relaxes stresses near the main crack tip and results in the formation of bulged metal-film ligaments which act to bridge the interfacial crack. Toughnesses exceeding that of the brittle glass can obtain whilst the main crack remains at the interface.

2. The fracture toughness in the presence of the patterned arrays shows marked, rising resistance-curve (R-curve) behavior with plateau toughness increases of one or two orders of magnitude compared to the inherent toughness ($G_o \sim 2$ J/m^2) of the plain glass/copper interfaces used. Such toughening behavior is ascribed primarily to the development of a zone behind the crack tip wherein plastic stretching of metal-film ligaments which bridge the interfacial crack provides crack-tip shielding. The greatest toughening has been observed in the limit that the ligaments stretch until they tear.

3. Subcritical, stress-corrosion crack-growth rates along interfaces near such microcrack arrays are orders of magnitude slower than along plain interfaces; apparent threshold interfacial fracture energies appear to be increased by factors comparable to those for the increase in G_c. Faster interfacial growth rates in humid atmospheres are attributed to environmentally induced weakening of interfacial bonds by adsorbing water molecules; this effectively limits the extent of the plastic stretching of bridging segments of metal film with passage of the crack.

4. Non-planar interfacial morophologies can enhance the fracture resistance by crack deflection which inhibits extension of the interfacial crack and, so, induces greater plastic stretching of the bridging metal ligaments as the main crack extends. The plastic deformation behavior of the metal, together with the size and spacing of the bridging ligaments, are also deemed to be important.

Acknowledgments: This work was supported by the Director, Office of Energy Research, Office of Basic Energy Sciences, Materials Sciences Div. of the U.S. Dept. of Energy under Contract No. DE-AC03-76SF00098. J. Crean, Dr. J. A. Wasynczuck, and G. Chan provided valuable assistance. Pattern-etched glass was prepared at the Microfabrication Laboratory in the EECS Dept.

REFERENCES

1. B. N. Chapman, J. Vac. Sci. Technol. **11**, 106-13 (1974).
2. A. J. Blodgett, Jr., Sci. Amer. **249**, 86-96 (1983).
3. V. V. Krstic, P. S. Nicholson, and R. G. Hoagland, J. Am. Ceram. Soc. **64**, 499-504 (1981).
4. A. G. Evans and R. M. McMeeking, Acta Metall. **34**, 2435-41 (1986).
5. H. L. Marcus, ASTM STP **907** (1986).
6. D. B. Marshall, B. N. Cox, and A. G. Evans, Acta Metall. **33**, 2013-21 (1985).
7. R. Marissen, in: Fatigue '87, Proc. 3rd. Intl. Conf. on Fatigue and Fatigue Thresholds, R. O. Ritchie and E. A. Starke, eds. (EMAS Ltd., Warley, U.K., 1987) p.1271
8. P. F. Becher and W. L. Newell, J. Mat. Sci. **12**, 90-6 (1977).
9. D. B. Marshall and A. G. Evans, J. Appl. Phys. **56**, 2632-8 (1984).
10. T. Suga and G. Elssner, Mat. Res. Soc. Symp. Proc. **40**, 203-10 (1985).
11. J. J. Mecholsky, in ASTM STP **855**, 324-36 (1985).
12. R. M. Cannon, V. Jayaram, B. J. Dalgleish, R. M. Fisher, Mat. Res. Soc. Symp. Proc. **72**, 121-26 (1986).
13. R. M. Cannon, V. Jayaram, B. J. Dalgleish, and R. M. Fisher, in: Ceramic Microstructures '86: Role of Interfaces, J. A. Pask and A. G. Evans, eds., (Plenum, New York, 1987) pp. 959-68.
14. T. S. Oh, R. M. Cannon, and R. O. Ritchie, J. Am. Ceram. Soc. **70**, C352-5 (1987).
15. D. E. Pitkanen and C. J. Speerschneider, IEEE Trans. **CHMT-4**, 250-6 (1981).
16. F. P. Bailey and K. J. T. Black, J. Mat. Sci. **13**, 1045-52 (1978).
17. J. R. Rairden, C. A. Neugebauer, and R. A. Siesbee, Met. Trans. **2**, 719-22 (1971).
18. J.T. Klomp, Mat. Res. Soc. Symp. Proc. 40, 381-91 (1985).
19. R. M. Cannon, T. S. Oh, J. A. Wasynczuk, V. Jayaram, and R. O. Ritchie, "Critical and Subcritical Crack Growth at Glass-Copper Interfaces," to be published Am Ceram Soc.
20. R. M. Cannon, T. S. Oh, J. Rödel, A. M. Glaeser, and R. O. Ritchie, J. Am. Ceram. Soc. Comm. **71**, in review (1988).
21. T. S. Oh, et al, "Ceramic/Metal Interfacial Crack Growth: Toughening by Controlled Microcracks and Interfacial Geometries," submitted Acta. Metall.
22. J. Rödel and A. M. Glaeser, J. Am. Ceram. Soc. **70**, C172-5 (1987).
23. C. M. Melliar-Smith, J. Vac. Sci. Technol. **13**, 1008-22 (1976).
24. J. M. Mochel, U.S. Pat. 2,968,578 (1961).
25. J.E. Srawley and B. Gross, Mater. Res. Stand. **7**, 155-62 (1967).
26. S. M. Wiederhorn, A. M. Shorb, and R. L. Moses, J. Appl. Phys. **39**, 1569-72 (1968).
27. J. R. Rice and G. C. Sih, J. Appl. Mech. **32**, 418-23 (1965).

28. G. Blackman, et al, to be published, Rev. Sci. Instr.
29. S. M. Wiederhorn and L. H. Bolz, J. Am. Ceram. Soc. **53**, 543-8 (1970).
30. C. A. O. Henning, F. W. Boswell, and J. M. Corbett, Acta Metall. **23**, 177-85 (1975).
31. B. Cotterell and J. R. Rice, Int. J. Fract. **16**, 155-69 (1980).
32. S. Suresh, Metall. Trans. **14A**, 2375-85 (1983).
33. G. V. Elmore and R. F. Hershberger, J. Electrochem. Soc. **121**, 107-8 (1974).
34. S. G. Stalnecker, Jr., U.S. Patent 3,296,012 (1967).
35. K. T. Faber and A. G. Evans, Acta Metall. **31**, 565-76 (1983).
36. M. D. Thouless, "Bridging and Damage Zones During Crack Growth," in press, J. Am. Ceram. Soc.
37. R. M. Cannon, R. M. Fisher, and A. G. Evans, Mat. Res. Soc. Symp. Proc. **54**, 799-804 (1986).
38. S.M. Wiederhorn, J. Am. Ceram. Soc. **52**, 99-105 (1969).

LAWRENCE BERKELEY LABORATORY
TECHNICAL INFORMATION DEPARTMENT
UNIVERSITY OF CALIFORNIA
BERKELEY, CALIFORNIA 94720